Acta Biochim Biophys Sin 2014, 46: 647–658 | © The Author 2014. Published by ABBS Editorial Office in association with Oxford University Press on behalf of the Institute of Biochemistry and Cell Biology, Shanghai Institutes for Biological Sciences, Chinese Academy of Sciences. DOI: 10.1093/abbs/gmu045.
Advance Access Publication 13 June 2014

Original Article

Expression analysis of BORIS during pluripotent, differentiated, cancerous, and non-cancerous cell states

Sara Soltanian[1,2], Hesam Dehghani[3,4*], Maryam M. Matin[1,2], and Ahmad Reza Bahrami[1,2]

[1]Department of Biology, Faculty of Science, Ferdowsi University of Mashhad 91779-48974, Mashhad, Iran
[2]Cell and Molecular Biotechnology Research Group, Institute of Biotechnology, Ferdowsi University of Mashhad, Mashhad 91779-48974, Iran
[3]Department of Basic Sciences, Faculty of Veterinary Medicine, Ferdowsi University of Mashhad, Mashhad 91779-48974, Iran
[4]Embryonic and Stem Cell Biology and Biotechnology Research Group, Institute of Biotechnology, Ferdowsi University of Mashhad 91779-48974, Mashhad, Iran
*Correspondence address. Tel: +98-(511)-880-5613; Fax: +98-(511)-876-3852; E-mail: dehghani@um.ac.ir

BORIS/CTCFL is an 11 zinc finger protein, which is the paralog of CTCF, a ubiquitously expressed protein with diverse roles in gene expression and chromatin organization. Several studies have shown that the expression of BORIS is restricted to normal adult testis, pluripotent cells, and diverse cancer cell lines. Thus, it is known as a cancer-testis (CT) gene that has been hypothesized to exhibit oncogenic properties and to be involved in cancer cell proliferation. On the contrary, other reports have shown that its expression is more widespread and can be detected in differentiated and normal somatic cells; hence, it might have roles in general cellular functions. The present study was aimed to analyze the expression of BORIS in different cell states of pluripotent, differentiated, cancerous and non-cancerous. We found that the two cell states of pluripotency and differentiation are not accompanied with significant variations of BORIS expression. Furthermore, *Boris* transcripts were detected at approximately the same level in cancer and non-cancer cell lines. These findings suggest that, in contrast to some previous reports, the expression of mouse BORIS is not limited to only cancerous cells or pluripotent cell states.

Keywords BORIS; differentiation; cancer; embryonal carcinoma P19 cells; retinoic acid

Received: February 27, 2014 Accepted: April 8, 2014

Introduction

Brother of the regulator of the imprinted site (BORIS) or CCCTC-binding factor-like protein (CTCFL) is an 11 zinc finger (ZF) protein, described as a transcriptional regulator. BORIS is a paralog of CCCTC-binding factor (CTCF), a protein that has been called the 'master weaver of the genome' [1–3]. BORIS exhibits high homology with CTCF in the central 11 ZF DNA binding domains, so it is thought to act as an antagonist to CTCF in normal and cancer cells by binding to the same target sequences [1]. Despite the high homology of central domains in CTCF and BORIS, the flanking N- and C-terminal domains show very little sequence homology, implying that BORIS and CTCF may recruit different cofactors and lead to various cellular outcomes [3–5].

BORIS was originally found in male germ cells, particularly in primary spermatocytes and round spermatids within the normal testis [4]. In addition, significant expression of BORIS was also detected in tumors and cancer cell lines [6–19]. The majority of these reports did not find the expression of BORIS in other normal somatic tissues and cells [4,6,8–10,18,20]. Thus, the expression of BORIS was viewed as an aberrant phenomenon in cancer, and its expression in testis and many cancers led to its classification as a cancer-testis (CT) gene [1,8,16,17]. In a few studies, BORIS expression was also detected in some pluripotent cells including human embryonic stem (hES) [18,21] and embryonal carcinoma (EC) cells (TERA-1, TERA-2, NTERA2, and NCCIT) [15]. These reports suggested a possible link between the state of pluripotency (undifferentiated) and BORIS expression. A pluripotent and an undifferentiated state in tumor cells may lead to self-renewal, high proliferative capacity, immortality, and phenotypic plasticity [22–25]. In fact, the stem cell-like phenotypes including the expression of pluripotent marker genes especially those associated with reprogramming, the undifferentiated and proliferative stem cell state, and also the maintenance of that state (accompanied by the expression of OCT4, SOX2, KIF4, and c-MYC) have been detected in cancer cells, especially in poorly differentiated aggressive tumors [26–39]. These evidence suggest that the acquisition of a stemness state, an important phase towards cancer [40], and the expression of BORIS might be interrelated. According to these reports, BORIS in cancer-pluripotent cells might replace CTCF on the regulatory regions of CT genes (e.g. *Oct4* and some members of MAGE-A family genes), oncogenes (e.g. *c-Myc*), and

hTERT promoter to disturb a silenced gene state and to lead to the proliferation of cancer cells [1,4,6,10,11,14,41–44].

On the contrary, the expression of BORIS cannot be detected in some cancer cell lines or tumors [10,12,15–17,45,46], and has also been detected in several mouse and human somatic tissues and non-cancerous cell lines [17,46,47]. This may point to the widespread expression of BORIS which is not restricted to cancerous cell lines. In addition, it has been found that the expression of some CT genes does not rely on the presence of BORIS [12,17,48,49], and thus, it is unlikely that BORIS would be a major CT gene inducing factor [50]. Furthermore, some more general biological functions including a regulatory role in normal cell division have been proposed for BORIS [47], which leads to a significant decrease in cell proliferation and clonogenic capacity. These growth inhibitory functions categorize BORIS as a candidate tumor suppressor gene, rather than an oncogene [20].

Reports indicating the expression of BORIS in cancer-pluripotent cells on one hand, and studies showing the widespread expression and function of BORIS in normal cells and tissues on the other hand, prompted us to identify whether the expression of this gene is restricted to a specific cell state, pluripotency vs. differentiated, and cancerous vs. non-cancerous. To this point in P19 cells, we quantified the level of BORIS during an undifferentiated pluripotent state (EC cells), in early differentiated retinoic acid (RA)-induced 4-day old embryoid bodies (EBs) (EB4), and in fully differentiated EBs (4 days after transfer to tissue culture plates in RA-free medium; EB-D4). In addition, we also quantified *Boris* in mouse cancer (CT26, N2A) and non-cancer (3T3, STO) cell lines. Along with the expression of BORIS, we also identified some pluripotency-associated factors [OCT4, NANOG, SSEA1, and alkaline phosphatase (AP)], and several differentiation markers (GATA-4, Tubulin βIII, NeuN, and Neurofilament 200). We found that the expression of BORIS does not show a significant change during the differentiation of P19 cells. In addition, *Boris* transcript was detected in both cancer (N2A and CT26) and non-cancer (STO) cell lines at approximately the same level. These findings indicate that a pluripotency state in either cancer or pluripotent cells may not be related to the level of BORIS expression and that the expression of BORIS is not altered due to the cancerous or non-cancerous state of the cells.

Materials and Methods

Culture and induction of differentiation of P19 cells

P19, STO, 3T3, N2A, and CT26 cells were obtained from Pasteur Institute (Tehran, Iran). P19 cells are EC pluripotent cells with the ability to differentiate to derivatives of three germ layers in response to different chemical inducers and culture conditions [51,52]. In response to RA treatment and EB formation, P19 cells lose their pluripotency rapidly, as evidenced by the decreased expression of pluripotent stem cell markers [53–55] and differentiate into neurons, glial, and fibroblast-like cells [56,57]. P19 cells were cultured in minimum essential medium eagle, alpha modification (α-MEM; Sigma-Aldrich, Munich, Germany) and STO, 3T3, N2A, and CT26 cells were cultured in Dulbecco's modified Eagle's medium (Gibco, Grand Island, USA). Both media were supplemented with 10% fetal bovine serum (FBS) and 1% penicillin-streptomycin (Gibco). All the cell lines were incubated at 37°C in a 5% CO_2 atmosphere.

For RA-induced differentiation of P19 cells, aggregates were formed by placing 0.2×10^6 cells into 8 cm diameter bacteriological grade petri dishes containing 8 ml of complete α-MEM medium supplemented with 0.5 μM RA (Sigma, Munich, Germany). After 2 days incubation, the medium was replenished with fresh RA-containing medium [57] and cells were cultured for two more days. EB4 were dissociated by trypsinization and their viability was assayed by trypan blue exclusion assay. For neurodifferentiation, EB4 aggregates were plated onto tissue culture grade surfaces in medium lacking RA and were cultured for additional 4 days (EB-D4). Media were replaced every 48 h [56]. RA was prepared as 10^{-2} M stock solutions in ethanol and was diluted directly into the culture medium to obtain the desired concentration. In this work, undifferentiated P19 cells, EB4, and the EB-D4 cells were studied.

AP staining

To detect AP activity in P19 cells and its alteration after RA treatment, P19 cells were grown on coverslips and were fixed with 4% paraformaldehyde (PFA; Sigma) in phosphate-buffered saline (PBS) for 10 min. For AP staining of aggregates (EB4), by using a plugged Pasteur pipette, an individual aggregate was transferred on the center of gelatin-coated glass coverslip placed in each well of a six-well tissue culture plate. To avoid dislodging the cells from the surface, 2 ml medium was added to each well. Incubation for a few hours allowed aggregates to attach to the gelatin surface. To investigate AP activity on mature differentiated cells (EB-D4), after 4 days in suspension, aggregates were transferred and cultured on the center of coverslips for 4 days in RA-free medium. Cells cultured on coverslips were fixed with 4% PFA. After fixation, each coverslip was washed three times with AP buffer (100 mM Tris-HCl, 100 mM NaCl, 5 mM $MgCl_2$, 0.05% Tween-20, pH 9.5, all from Merck, Ballerup, Denmark), and then was covered with 1 ml of AP solution prepared by mixing 120 ml of 1% 5-bromo-4-chloro-3-indolyl phosphate (Fermentas, Schwerte, Germany) in 100% dimethylformamide (DMF; Merck), 120 ml of 1.5% nitroblue tetrazolium (Fermentas) in 70% DMF, and 5 ml of AP buffer. After 15 min, coverslips were washed with AP buffer, then mounted on the slide with the application of 40 μl antifade, and observed under an Olympus BX-UCB microscope (Olympus, Tokyo, Japan).

Immunocytochemistry

Immunocytochemistry (ICC) was used to detect the presence of pluripotency and neural cell-specific proteins. Cells were fixed as described for AP staining. After fixation and washing with PBS (three times, 5 min each), cells were permeabilized with Tris-buffered saline containing 0.5% Triton X-100 (Merck) for 10 min at room temperature (RT). Cells were then washed with PBS (three times, 5 min each) and endogenous peroxidase was blocked by incubating in 3% H_2O_2 (Sigma) in PBS for 30 min. After washing with PBS, blocking of non-specific binding was performed by incubation in 4% (v/v) bovine serum albumin (BSA; Invitrogen, Grand Island, USA) for 45 min. Cells were then incubated with the specific primary antibodies: mouse anti-BORIS (Cat. No. 061502E05, 1 : 50; Absea Biotechnology Ltd, Beijing, China), mouse anti-OCT4 (Cat. No. sc-5279, 1 : 100; Santa Cruz Biotechnology, Inc., Heidelberg, Germany), mouse anti-NANOG (Cat. No. sc-293121, 1 : 500; Santa Cruz Biotechnology, Inc.), mouse anti-SSEA1 (Cat. No. sc-101462, 1 : 100; Santa Cruz Biotechnology, Inc.), and rabbit anti-Neurofilament 200 (Cat. No. N4142, 1 : 100; Sigma-Aldrich) in blocking buffer (1% BSA) overnight at 4°C. Then, cells were washed with PBS (three times, 10 min each) and were incubated for 1 h at RT with secondary antibodies specific for each primary antibody: goat anti-rat IgG-HRP (Cat. No. sc-2065, 1 : 500; Santa Cruz Biotechnology, Inc.), goat anti-mouse IgG2b-HRP (Cat. No. ab97250, 1 : 500; Abcam, Cambridge, UK), goat anti-mouse IgG1-HRP (Cat. No. ab97240, 1 : 1000; Abcam), rat anti-mouse IgM-HRP (Cat. No. 04-6820, 1 : 1500; Invirogen), and donkey anti-rabbit IgG-HRP (Cat. No. sc-2317, 1 : 500; Santa Cruz Biotechnology, Inc.). Finally, cells were washed for several times with PBS and stained with 3,3′-diaminobenzidine (Cat. No. D8001; Sigma-Aldrich) at RT for 2 min. After washing with PBS, coverslips were mounted on the slide with the application of 40 μl antifade and were analyzed under the Olympus BX-UCB microscope. Negative controls were stained with only the secondary antibodies.

RNA extraction and cDNA synthesis

Total RNA was isolated using Total RNA isolation kit (DENAzist Asia, Mashhad, Iran) according to the manufacturer's guidelines. The quantity and quality of RNA were assessed using a Nanodrop 2000 spectrophotometer (Thermo Scientific, Wilmington, USA) and agarose gel electrophoresis (**Supplementary Fig. S1**).

Possible contaminating genomic DNA was removed by DNase I treatment. For DNase I treatment, 10–50 μg of total RNA was digested for 15 min at RT with 1 μl (10 U/μl) of DNase I (Roche, Penzberg, Germany) and 1× DNase I reaction buffer in a 50 μl reaction volume. First-strand cDNA was prepared in a total volume of 20 μl containing 1 μg total RNA, 0.5 μg Oligo(dT)$_{18}$ primer (Thermo Scientific), 1× RT buffer (Thermo Scientific), 1 mM dNTPs (Genet Bio, Inc., Daejeon, Korea), and 200 U of reverse transcriptase (Thermo Scientific). The reaction was incubated at 42°C for 60 min. Negative control reactions were carried out without the use of reverse transcriptase.

Polymerase chain reaction

The polymerase chain reaction (PCR) mixture (25 μl) contained 1 μl of template cDNA, 0.04 U of *Taq* DNA polymerase (Genet Bio, Inc.), 1× PCR buffer, 1.5 mM $MgCl_2$, 0.2 mM dNTPs, and 200 nM of each primer. The number of PCR cycles in semi-quantitative reverse transcription-PCR (RT-PCR) has been adjusted for each gene to prevent reaching a saturation level and normalization with respect to *L37* cDNA allows to estimate the relative abundance of each target mRNA. Primers for *L37*, *Oct4*, *Nanog*, *Gata-4*, *NeuN*, and *Boris* were chosen from different intron-spanning exons. All primers were the same for both conventional and real-time quantitative PCR (qPCR). All specific primers are described in **Table 1** and **Supplementary Fig. S2**.

Quantitative real-time RT-PCR

To quantify the level of transcripts for *Oct4*, *Nanog*, and *Boris*, quantitative RT-PCR was performed. The reactions contained 1× SYBR Green Real-time PCR Master Mix (Pars Tous, Mashhad, Iran), 2 μl diluted cDNA template and each primer at 250 nM in a 20 μl reaction volume, which was carried out on a CFX-96 Thermo cycler (Bio-Rad, Hercules, USA). Gene-specific primers were designed using Oligo7 Primer Analysis Software. Amplification conditions for *Oct4*, *Nanog*, and *L37* were: 95°C for 10 min, followed by 40 cycles of 95°C for 30 s, 60°C for 30 s, and 72°C for 30 s. Plate read step to collect fluorescence for mentioned genes was at 72°C. The same program was used for *Boris* except that annealing temperature was 62°C and there was an extra step of 78°C for 10 s to collect fluorescence at a temperature above the melting point of any possible primer dimers. At the end of the PCR runs to derive melting curves, temperature was increased in steps of 1°C for 10 s from 60°C to 95°C.

Analysis of melting curves clearly indicated that each of the primer pairs described in **Table 1** amplified a single expected product with a distinct T_m (**Supplementary Fig. S3**). The accuracy of the amplification reaction was validated by gel electrophoresis and restriction digestion of PCR products (**Supplementary Fig. S4**) and sequencing.

For undifferentiated P19 cells and each stage of differentiated cells (EB4 and EB-D4), three biological replicates were considered. Three series of isolated RNAs were subjected to cDNA synthesis and qPCR. For each sample, qPCR readings were performed in triplicate and the mean value of each triplicate was used for the calculation of the mRNA expression levels. To acquire the highest level of accuracy, the real-time PCR analyses were performed in two series of experiments.

Table 1. Primers used in RT-PCR and real-time qPCR

Gene	Primer sequence (5′→3′)	Annealing temperature (°C)	Product length (bp)
POU domain, class 5, transcription factor 1 (*Oct4*)	F: CTCTGAGCCCTGTGCCGACC	60	202
Accession number: NM_013633.3	R: CTGAACACCTTTCCAAAGAGAACGC		
Nanog homeobox (*Nanog*)	F: GAACTCTCCTCCATTCTGAACCTG	60	137
Accession number: NM_028016.2	R: GGTGCTGAGCCCTTCTGAATC		
CCCTC-binding factor (ZF protein)-like (*Ctcfl*) (*Boris*)	F: ACCTGAGGAAGTACCATGACCCGAA	62	196
Accession number: NM_001081387.2	R: TTGTGTCCTGCTTCTCCCTCCGA		
Ribosomal protein L37 (*Rpl37*)	F: GGTGCTTTCTCTTCCGGTCT	60	250
Accession number: NM_026069.3	R: TCTTTAGGTGCCTCATCCGACCAG		
GATA binding protein 4 (*Gata-4*)	F: GAAAACGGAAGCCCAAGAACC	58	186
Accession number: NM_008092.3	R: TGCTGTGCCCATAGTGAGATGAC		
Tubulin, beta 3 class III (*Tubb3*)	F: CTGTCCGCCTGCCTTTTCG	67	589
Accession number: NM_023279.2	R: TAGGGCTCCACCACAGTGTCC		
Fox-1 homolog (*Caenorhabditis elegans*) 3 (*Rbfox3*) (*NeuN*)	F: CAACATCCCCTTCCGGTTC	59	200
	R: TGACCTCAATTTTCCGTCCC		
Accession number: NM_001039167.1(Variant 1)			
Accession number: NM_001039168.1(Variant 2)			
Accession number: NM_001024931.2 (Variant 3)			

PCR efficiencies (E) were calculated for all used primers from the given slopes of standard curves, generated using 5 fold serially diluted solutions of positive control cDNA samples, according to the following equation: $E = (10^{-1/\text{slope}} - 1) \times 100\%$. Positive control for *Boris* expression was mouse testis, and P19 cells were used as a positive control for *L37*, *Oct4*, and *Nanog*. All standard curves were linear in the analyzed range with an acceptable correlation coefficient (R^2). For standard curves and parameters of a standard curve for each gene see **Table 2** and **Supplementary Fig. S5**.

In this study, the variability of *L37* transcript levels was evaluated before and after RA treatment by real-time PCR. The mean threshold cycle (C_T) of *L37* was similar in undifferentiated P19 cells, EB4, and EB-D4 (**Supplementary Fig. S6**). Therefore, we found *L37* as a suitable internal control in these experiments.

Standard curve method for relative quantification

This method is often applied when the amplification efficiencies of the reference and target genes are unequal [58,59]. *L37* was selected as a reference gene so that the expression of the gene of interest was quantified relative to *L37* expression. Required calculations in this method included the followings: (i) calculation of averages for triple readings; (ii) normalization of the quantity of the target gene by dividing it to the quantity of the reference gene (*L37*) in the test (treated P19 cells) and calibrator groups (untreated P19 cells); and (iii) dividing the normalized quantities of the test over those in the calibrator group to determine *n*-fold difference.

Table 2. Evaluation of parameters of a standard curve for each gene

Target	Slop	R^2	Efficiency (%)
L37	−3.315	0.996	100.2
OCT4	−3.308	0.993	100.5
NANOG	−3.320	0.990	100.0
BORIS	−3.330	0.991	101.0

Efficiency $= (10^{-1/\text{slope}} - 1) \times 100\%$.

Comparative C_T method for relative quantification

This method is applied when amplification efficiencies of the target and reference genes are similar and close to 100%. Since our results met these criteria, we analyzed our qPCR data using this method, too. This analysis method involves a calculation known as the Delta Delta C_T ($\Delta\Delta C_T$), which is based on a C_T number comparison between the target gene and the reference gene relative to a calibrator. The data were analyzed using the following equation [60]:

$$\text{Relative quantity} = 2^{-\Delta\Delta C_T}$$

$$\Delta\Delta C_T = (C_{T,\text{Target gene}} - C_{T,\text{Reference gene}})_{\text{Test sample}} - (C_{T,\text{Target gene}} - C_{T,\text{Reference gene}})_{\text{Calibrator sample}}$$

The fold change in the target gene relative to the calibrator sample was calculated for each sample using the above-mentioned equation.

Western blot analysis

Western immunoblotting was used to verify specificity of anti-mouse BORIS antibody. For this test, mouse testis tissue was used as a positive control for BORIS expression. Testis tissue was immediately frozen in liquid nitrogen, homogenized with a mortar and pestle, and then suspended in lysis buffer [50 mM Tris-HCl, 5 mM ethylenediaminetetraacetic acid, 2% sodium dodecyl sulfate (SDS)]. After incubation on ice, lysate was centrifuged (13,000 *g*, 15 min) and supernatants were collected. Tissue lysates were heated at 95°C for 5 min, resolved by SDS–polyacrylamide electrophoresis and then transferred to polyvinylidene difluoride membranes. Membranes were incubated in a blocking solution containing 5% dry milk and 0.1% Tween-20 in PBS (overnight at 4°C) and then with primary mouse anti-BORIS antibody (Cat. No. 061502E05, 1 : 1000) for 1 h at RT. Antibody binding was revealed by incubation with goat anti-rat IgG-HRP (Cat. No. sc-2065, 1 : 10,000) for 1 h at RT. The ECL Plus immunoblotting detection system (GE Healthcare Biosciences, Buckinghamshire, UK) was used to detect HRP activity on a chemiluminescence detector system (G Box; Syngene, Cambridge, England).

Flow cytometry

To examine the expression of BORIS as intracellular antigen by flow cytometry (FCM), the following protocol was employed. Cells were dissociated with trypsin and then washed by centrifugation with washing buffer (PBS and 5% FBS). Cells were then fixed with 4% PFA and permeabilized with 0.5% Triton-X-100. After two washing, cells were incubated with diluted primary mouse anti-BORIS antibody (Cat. No. 061502E05, 1 : 50) for 45 min on ice and washed twice with washing buffer. Cells were then incubated with goat anti-rat IgG secondary antibody conjugated to Alexa Fluor® 546 (Cat. No. A-11081, 1 : 150; Life Technologies, Grand Island, USA) for 45 min on ice. At the end of the procedure, unbounded antibodies were removed by two times washing. Finally, cells were suspended in 0.5 ml of washing buffer and then analyzed by FACS callibur (BD Biosciences, San Jose, CA, USA). Negative control was incubated with the secondary antibody only.

Statistical analysis

Statistical analyses were carried out by one-way analysis of variance and paired *t*-test using SPSS version 11 software. Results were reported as mean ± SD and $P < 0.05$ was considered to be statistically significant.

Results

BORIS expression remains unchanged during RA-induced differentiation of P19 cells

Culture of EC P19 cells in non-tissue culture plates (bacterial petri dishes) in the presence of RA for 4 days resulted in the formation of tight rounded aggregates (EB4) (**Fig. 1A,B**) [56,61,62]. By plating EB4 aggregates on tissue culture dishes in a medium lacking RA, within 24 h fibroblast-like cells migrated out of the periphery of EB4 and attached to the dish. After 4 days of plating, neuron-like cells (EB-D4) appeared and grew rapidly over fibroblast-like cells (**Fig. 1C,D**) [52,56,57,63,64]. *Oct4* transcript level in RA-induced differentiated cells (EB4 and EB-D4) was <5% of that in untreated P19 cells (**Fig. 2A**) and transcription of *Nanog* showed 81% and 87% decrease in EB4 and EB-D4, respectively (**Fig. 2B**). In contrast to the sharp decrease in the expression of pluripotency genes during RA-induced differentiation, the transcription of *Boris* did not alter significantly (**Fig. 2C**). Two methods of relative quantification of transcript levels based on standard curve and comparative C_T resulted in similar results (**Table 3**).

Loss of pluripotency in P19 cells in response to RA treatment was also evident at protein level by the decreased expression of pluripotency markers and up-regulation of differentiation markers [52,53]. OCT4 and NANOG are well-known pluripotency genes that are required to maintain the pluripotency and self-renewal of pluripotent cells [65–68]. These two markers and SSEA1 that are highly expressed in pluripotent mouse EC cells (including P19 cells) were rapidly down-regulated at protein level during RA-induced differentiation (**Fig. 3** and **Supplementary Fig. S7**) [53,55,69–72]. Down-regulation of OCT4 was also shown by western blotting (**Supplementary Fig. S8A**). In addition, the AP activity of undifferentiated P19 cells was also decreased during differentiation (**Supplementary Fig. S9**) [53,54,73,74]. In EBs,

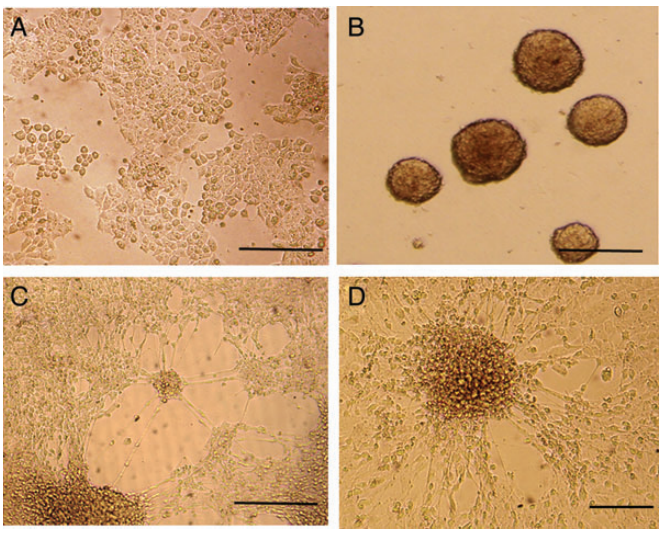

Figure 1. Morphologies of P19 cells after RA treatment The undifferentiated EC cells grow while attached to the surface of tissue culture dish (A). EB4 were formed when P19 cells were plated as single-cell suspension in bacterial petri dish in the presence of RA for 4 days (B). A few fibroblast and many neuron-like cells migrated out of EB4 cells which were plated in tissue culture dishes in a medium lacking RA for 4 days (C and D). Scale bars, 250 μm (A–C) or 100 μm (D).

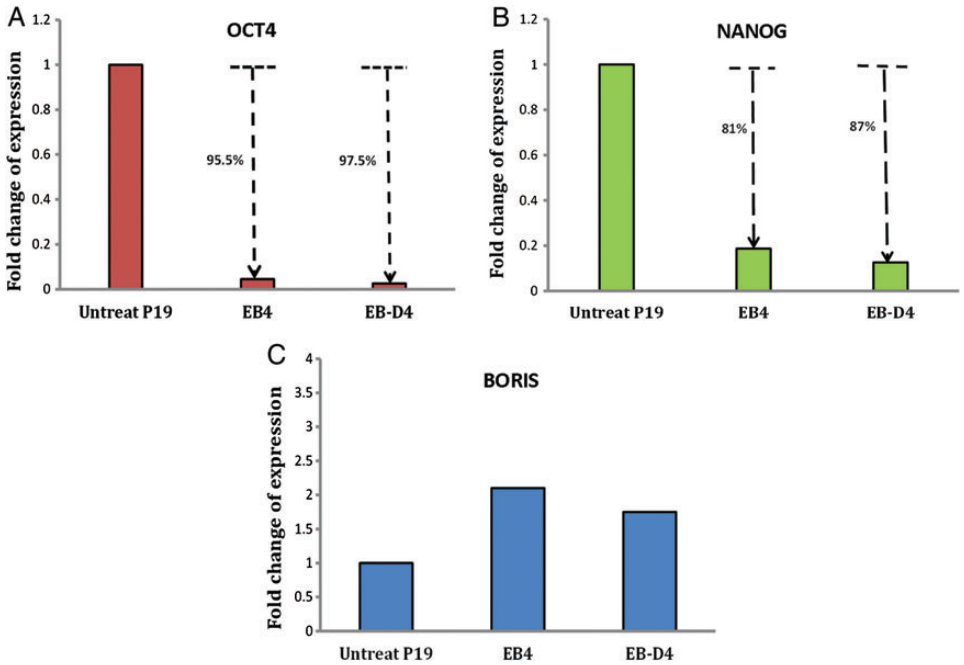

Figure 2. Comparative real-time PCR results Fold changes for *Oct4* (A), *Nanog* (B), and *Boris* (C) genes during RA-induced differentiation of P19 cells. *Y*-axis represents the fold change in transcript levels compared with RA-untreated P19 cells (designated as 1.0). Expression of *Oct4* showed a 95.5% drop in EB4 and 97.5% drop in EB-D4. *Nanog* expression in EB4 and EB-D4 showed 81% and 87% decrease, respectively. *Boris* expression remains unchanged (statistically not significant) during RA-induced differentiation of P19 cells.

Table 3. Relative quantitative value of target gene using standard curve and comparative $\Delta\Delta C_T$ methods

Gene	Stage EB4		Stage EB-D4	
	$2^{-\Delta\Delta C_T}$	Normalized test group/normalized calibrator group	$2^{-\Delta\Delta C_T}$	Normalized test group/normalized calibrator group
OCT4	0.055	0.044	0.026	0.025
NANOG	0.2	0.16	0.16	0.13
BORIS	2.1	3.0	1.5	2.0

pluripotent markers are expressed in the outer differentiated cells and a few undifferentiated EC cells that are localized in the inner core. Differentiation of P19 cells into endoderm and neuron cells was further confirmed by over-expression of differentiation markers including *Gata-4* (endoderm) [75], *Tubulin βIII* (ectoderm), *NeuN* (ectoderm), and Neurofilament (neuron intermediate filament) (**Fig. 4**) [54,56,76–84].

Expression of BORIS protein was detected in undifferentiated and differentiated P19 cells (EB4 and EB-D4) by ICC (**Fig. 5**). For quantitative analysis, expression of BORIS was also characterized by FCM. Almost 74% of undifferentiated P19 cells were BORIS positive (**Fig. 6A**). Similar results were obtained with EB-D4 (**Fig. 6B**). Therefore, differentiation did not significantly alter the number of BORIS-positive cells. Although the antibody used in this investigation was previously characterized for their specificity for BORIS [85], we verified specificity of BORIS antibody by western blotting, where a densely stained band of 70 kDa in mouse testis corresponded to theoretical molecular weight of mouse BORIS (**Supplementary Fig. S8B**).

BORIS expression in cancer and non-cancer mouse cells

Real-time RT-PCR analysis to compare the transcript levels of *Boris* in mouse cancer (CT26 and N2A) and non-cancer (STO and 3T3) cell lines revealed that except in 3T3 cells (with the highest level of expression), all other examined cell lines have similar levels of *Boris* mRNA (**Fig. 7A**). Testis as a positive control showed the highest level of *Boris* mRNA as previously described [4], while primary cell culture of mouse embryonic fibroblasts (MEFs) showed no expression of BORIS at mRNA and protein levels (**Fig. 7A,F**). Immunocytochemical staining of CT26, N2A, STO, and 3T3 cell lines revealed BORIS expression at protein level (**Fig. 7B–E**).

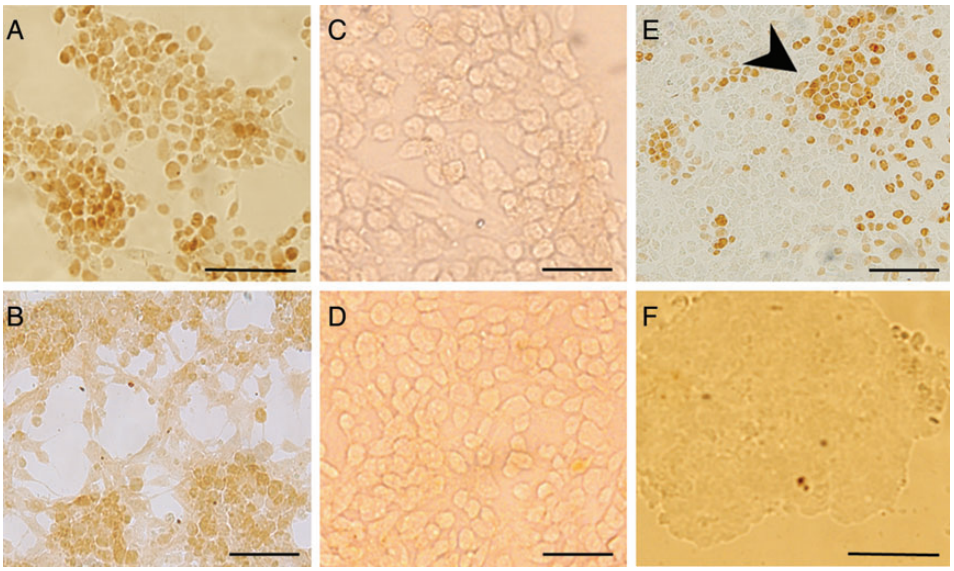

Figure 3. The expressions of OCT4 and NANOG were down-regulated during RA-induced P19 cell differentiation Staining of OCT4 in undifferentiated P19 cell (A), EB4 trypsinized into single cells (C), and EB-D4 (E). Staining of NANOG in undifferentiated P19 cell (B), EB4 trypsinized into single cells (D), and EB-D4 (F). A few OCT4-positive undifferentiated P19 cells in the core of EB-D4 (E) are indicated by arrow. Positive cells showed dark brown color, while after differentiation, cells do not express pluriopotency markers and thus, they are not stained and appear colorless. Scale bars, 250 μm (A and F) or 100 μm (B–E).

Discussion

Our findings reveal that: (i) the expression level of BORIS does not significantly change during differentiation of pluripotent mouse EC P19 cells, and (ii) *Boris* is expressed in cancer and non-cancer cell lines at approximately the same level. Therefore, the expression of this gene is not limited to cancer or pluripotent cells. Quantitative expression analysis of BORIS during RA-induced differentiation of pluripotent P19 cells did not show any significant variation at mRNA and protein levels (**Figs. 2C** and **6**) and immunostaining of BORIS in undifferentiated P19 cells, EB4, and EB-D4 showed expression of BORIS in both pluripotent and differentiated cells (**Fig. 5**). Therefore, down-regulation of pluripotent markers during RA-induced differentiation of pluripotent P19 cells does not lead to down-regulation of BORIS. In another research with similar results, it has been found that BORIS protein is co-localized with OCT4 and NANOG proteins in the nucleus of the majority of ES cells, and it continues to be expressed by some of the differentiating ES cells that have lost the expression of these two genes [21].

In our experiments, the loss of pluripotency marked by down-regulation of pluripotency markers (i.e. OCT4, NANOG, SSEA1, and AP) and differentiation into endoderm–neural lineage evidenced by elevated expression of differentiation markers (i.e. *Gata-4*, *NeuN*, *Tubulin βIII*, and Neurofilament 200). Our RT-qPCR results showed that during RA induction, transcript level of *Oct4* and *Nanog* dropped to <5% and 20% of those in untreated P19 cells, respectively (**Fig. 2A,B**). Furthermore, the ICC expression analysis showed down-regulation of pluripotency markers (e.g. OCT4, NANOG, SSEA1, and AP) in RA-induced EBs (EB4 and EB-D4) (**Fig. 3**, **Supplementary Figs. S7** and **S10**) and expression of neuron-specific marker Neurofilament 200 in EB-D4 (**Fig. 4D,E**). It is well documented that NANOG and OCT4 which are required to maintain the pluripotency and self-renewal of pluripotent cells [65,66,71,86–88], become down-regulated during RA-induced differentiation of pluripotent cells [53,55,71,89–91]. SSEA1 and AP are also two cell surface markers of mouse pluripotent cells that are down-regulated during differentiation [53,54,74].

RT-qPCR analyses in a series of cancer (CT26 colon carcinoma and N2A Neuroblastoma) and non-cancer (STO and 3T3 fibroblasts) cell lines showed that except in 3T3 cells that express the highest level of *Boris*, all other examined cell lines have similar levels of *Boris* mRNA, indicating that the state of cancerous or non-cancerous is not a determining factor for the level of *Boris* expression (**Fig. 7**). Several reports indicated that the expression of BORIS is not dependent on the cancerous or non-cancerous nature of cells and tissue. For example, although BORIS has been classified as a CT antigen, but new findings in melanoma, ovarian, prostate, breast, head and neck squamous cell carcinomas, and bladder carcinomas [12,15–17,46] have shown that BORIS expression may not directly correlate with tumorigenicity. These studies reported that *Boris* expression in primary melanomas (27%) is not as frequent as originally estimated for melanoma cell lines (90%) [17], and when measured quantitatively, levels in tumors were not statistically different from those in normal prostate, bladder, and ovarian tissues [15,16]. The elevated

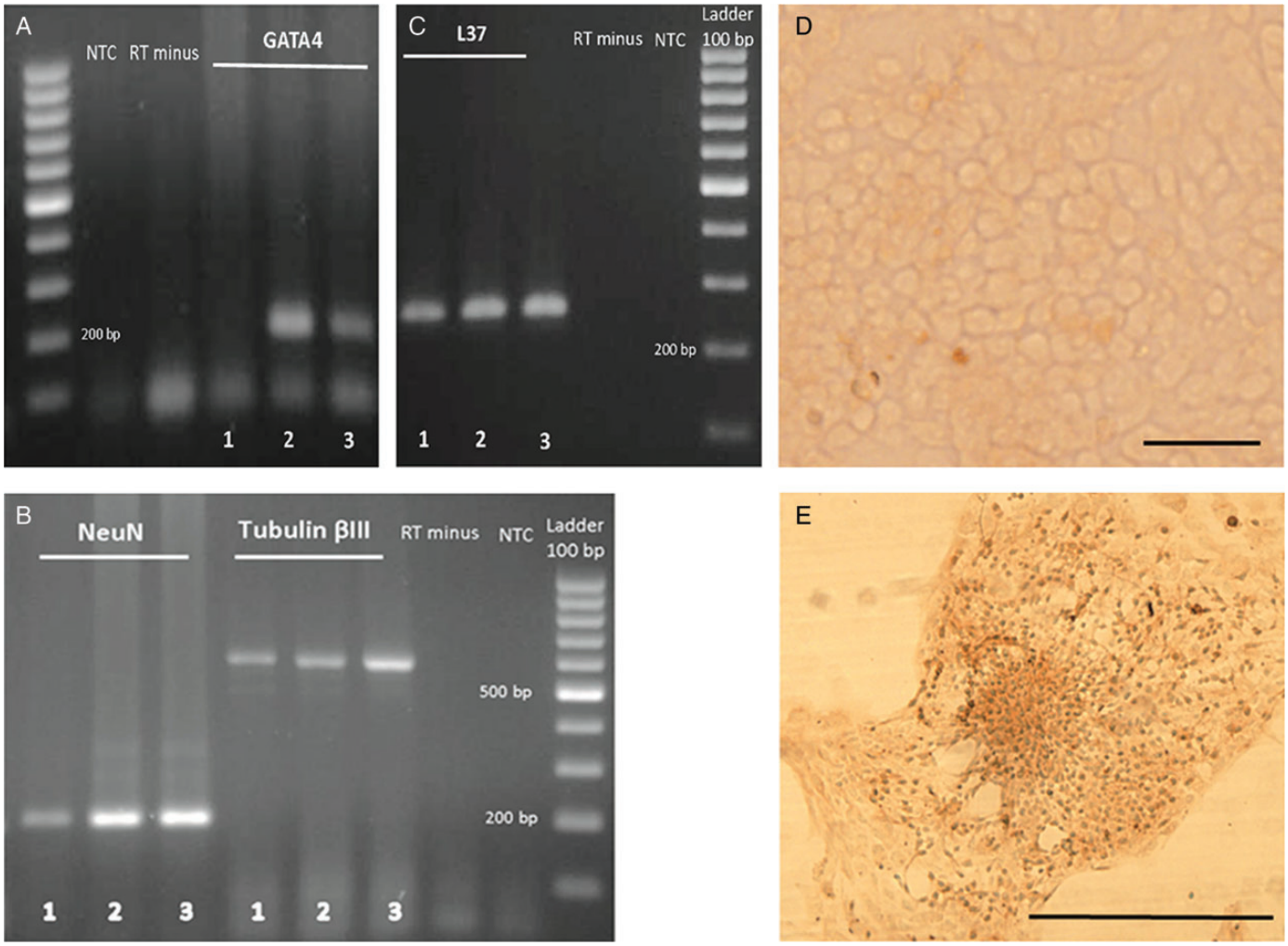

Figure 4. Expression analysis of lineage-specific genes during RA-induced differentiation of P19 cells The mRNA levels of endodermal (*Gata-4*) (A) and ectodermal (*Tubulin βIII* and *NeuN*) genes (B) in undifferentiated P19 cells (line designated with 1), EB4 (line designated with 2), and EB-D4 (line designated with 3) were determined by semi-quantitative RT-PCR. PCR amplification of the *L37* gene serves as an internal control for integrity of cDNA in each sample (C). Negative control lanes are indicated as RT minus (no reverse transcriptase for the reverse transcription reaction) and NTC (no-template control for the PCR reaction). Immunocytochemical analysis showed that undifferentiated P19 cells do not express Neurofilament 200 (D), while expression of this marker was detected in EB-D4 (E). Scale bars, 100 μm (D) or 1 mm (E).

expression of BORIS in several breast cancer cell lines and in the majority of primary breast tumors identified in one study has not been confirmed by another report [8,45]. Furthermore, some researchers have shown the expressions of different *Boris* isoforms in some normal tissues (e.g. skin, colon, kidney, ovary, fetal tissues, etc.) and non-cancer cells from various origins [4,17,18,46,47,92].

In agreement with the previous reports [6,8,10,20], we also found that BORIS is not expressed in primary-derived MEFs (**Fig. 7**). Primary cells such as MEFs have limited lifespan. After a certain number of population doublings, cells undergo the process of senescence and stop dividing. Therefore, they would normally not proliferate indefinitely. On the contrary, immortalized cell lines (e.g. STO, 3T3, CT26, and N2A) have evaded normal cellular senescence and have acquired the ability to proliferate indefinitely either through random mutation or deliberate modification. It has been reported that long-term maintenance of hES cells and indefinite division of cancer cells in culture are associated with chromosomal abnormalities such as loss of the q arm of chromosome 16 (the locus of CTCF) and gain of chromosome 20q13 (the genetic location of BORIS) and finally increased the levels of BORIS expression [93,94]. We propose that a similar association can be seen in other immortalized cell lines (e.g. STO, 3T3, CT26, and N2A) that undergo many rounds of cell division and probably chromosomal abnormalities. Therefore, we speculate that BORIS might be expressed in all type of cell lines, regardless of a cancerous or non-cancerous nature.

In conclusion, in this study, we provide evidence that the expression of BORIS does not change during differentiation of pluripotent P19 cells. Moreover, *Boris* is expressed at approximately the same level in cancer and non-cancer cell lines. Thus, the expression of BORIS may not be limited to cancerous and pluripotent cells.

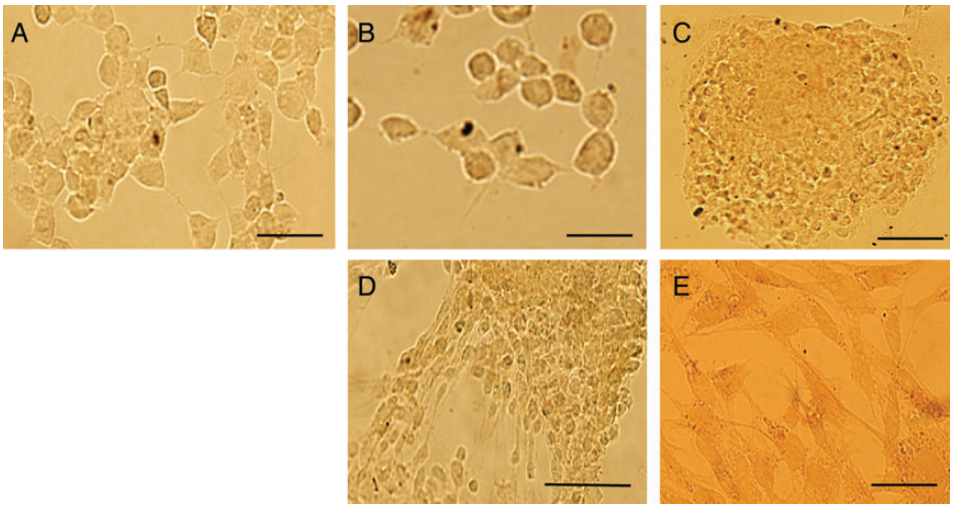

Figure 5. BORIS immunostaining of P19 cells during RA-induced differentiation Staining of BORIS protein in undifferentiated P19 cells (A), EB4 trypsinized into single cells (B), intact EB4 (C), and EB-D4 (D and E). Scale bars, 100 μm (A–C and E) or 250 μm (D).

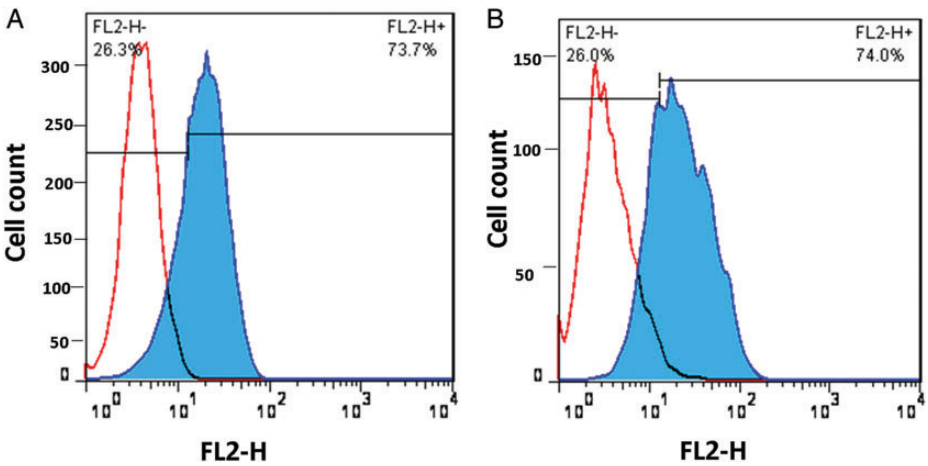

Figure 6. Expression analysis of BORIS during RA-induced differentiation of P19 cells FCM was used to identify the percentage of BORIS-positive cells in undifferentiated P19 (A; 73.7%) and EB-D4 (B; 74%) cells. Colored peaks show BORIS-positive cells, while white peaks represent negative controls (fluorescent signals obtained with the secondary antibody only).

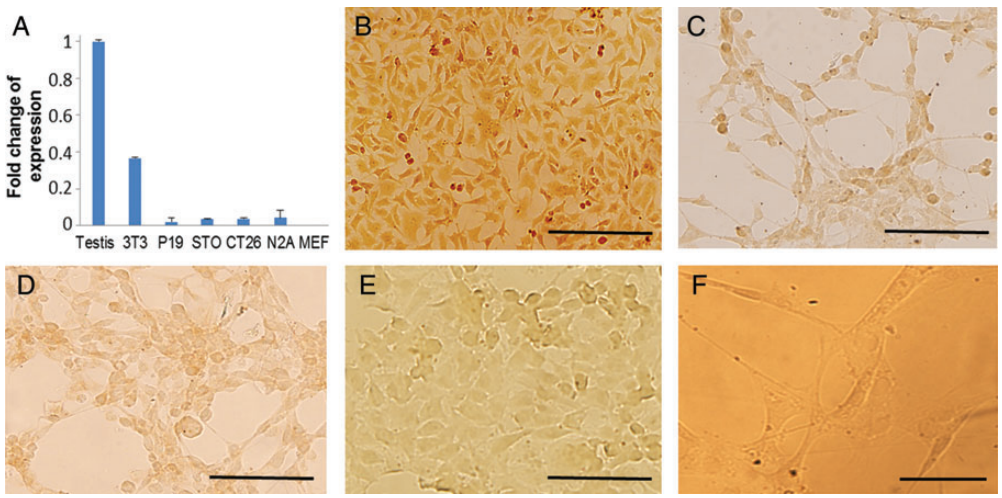

Figure 7. Expression of *Boris* mRNA analyzed by RT-qPCR and normalized to L37 Data are represented as fold change relative to the highest *Boris/L37* ratio (testis designated as 1.0). Two different RNA samples were used for each sample. Error bars indicate the standard deviation from two different experiments (A). Immunocytochemical detection of BORIS in mouse cell lines of 3T3 (B), STO (C), CT26 (D), N2A (E), and MEFs (F). Scale bars, 250 μm (B–E) or 100 μm (F).

Supplementary Data

Supplementary data are available at *ABBS* online.

Acknowledgements

The authors thank Dr Elena M. Pugacheva at National Institutes of Health (NIH) for generously providing BORIS expressing vectors, Dr Fatemeh B. Rassouli at Institute of Biotechnology, Ferdowsi University of Mashhad, Mashhad, Iran for the technical assistance, Dr Mohammad Mehdi Yaghoubi at International Center for Science, High Technology & Environmental Science, Kerman, Iran, for providing Neurofilament 200 antibody, and Dr Abdolreza Varaste at Mashhad University of Medical Sciences, Mashhad, Iran for laboratory equipment.

Funding

This work was supported by a grant from the Iranian Council of Biotechnology administrated by Institute of Biotechnology, Ferdowsi University of Mashhad, Mashhad, Iran (grant number 56894, to H.D.).

References

1. Klenova EM, Morse HC, III, Ohlsson R and Lobanenkov VV. The novel boris+ctcf gene family is uniquely involved in the epigenetics of normal biology and cancer. Semin Cancer Biol 2002, 12: 399–414.
2. Phillips JE and Corces VG. Ctcf: master weaver of the genome. Cell 2009, 137: 1194–1211.
3. Ohlsson R, Lobanenkov V and Klenova E. Does ctcf mediate between nuclear organization and gene expression? Bioessays 2010, 32: 37–50.
4. Loukinov DI, Pugacheva E, Vatolin S, Pack SD, Moon H, Chernukhin I and Mannan P, *et al*. Boris, a novel male germ-line-specific protein associated with epigenetic reprogramming events, shares the same 11-zinc-finger domain with ctcf, the insulator protein involved in reading imprinting marks in the soma. Proc Natl Acad Sci USA 2002, 99: 6806–6811.
5. Campbell AE, Martinez SR and Miranda JJ. Molecular architecture of ctcfl. Biochem Biophys Res Commun 2010, 396: 648–650.
6. Vatolin S, Abdullaev Z, Pack SD, Flanagan PT, Custer M, Loukinov DI and Pugacheva E, *et al*. Conditional expression of the ctcf-paralogous transcriptional factor boris in normal cells results in demethylation and derepression of mage-a1 and reactivation of other cancer-testis genes. Cancer Res 2005, 65: 7751–7762.
7. D'Arcy V, Abdullaev ZK, Pore N, Docquier F, Torrano V, Chernukhin I and Smart M, *et al*. The potential of boris detected in the leukocytes of breast cancer patients as an early marker of tumorigenesis. Clin Cancer Res 2006, 12: 5978–5986.
8. D'Arcy V, Pore N, Docquier F, Abdullaev ZK, Chernukhin I, Kita GX and Rai S, *et al*. Boris, a paralogue of the transcription factor, ctcf, is aberrantly expressed in breast tumours. Br J Cancer 2008, 98: 571–579.
9. Risinger JI, Chandramouli GV, Maxwell GL, Custer M, Pack S, Loukinov D and Aprelikova O, *et al*. Global expression analysis of cancer/testis genes in uterine cancers reveals a high incidence of boris expression. Clin Cancer Res 2007, 13: 1713–1719.
10. Hong JA, Kang Y, Abdullaev Z, Flanagan PT, Pack SD, Fischette MR and Adnani MT, *et al*. Reciprocal binding of ctcf and boris to the ny-eso-1 promoter coincides with derepression of this cancer-testis gene in lung cancer cells. Cancer Res 2005, 65: 7763–7774.
11. Smith IM, Glazer CA, Mithani SK, Ochs MF, Sun W, Bhan S and Vostrov A, *et al*. Coordinated activation of candidate proto-oncogenes and cancer testes antigens via promoter demethylation in head and neck cancer and lung cancer. PLoS One 2009, 4: e4961.
12. Cuffel C, Rivals JP, Zaugg Y, Salvi S, Seelentag W, Speiser DE and Lienard D, *et al*. Pattern and clinical significance of cancer-testis gene expression in head and neck squamous cell carcinoma. Int J Cancer 2011, 128: 2625–2634.
13. Renaud S, Pugacheva EM, Delgado MD, Braunschweig R, Abdullaev Z, Loukinov D and Benhattar J, *et al*. Expression of the ctcf-paralogous cancer-testis gene, brother of the regulator of imprinted sites (boris), is regulated by three alternative promoters modulated by cpg methylation and by ctcf and p53 transcription factors. Nucleic Acids Res 2007, 35: 7372–7388.
14. Kang Y, Hong JA, Chen GA, Nguyen DM and Schrump DS. Dynamic transcriptional regulatory complexes including boris, ctcf and sp1 modulate ny-eso-1 expression in lung cancer cells. Oncogene 2007, 26: 4394–4403.
15. Hoffmann MJ, Muller M, Engers R and Schulz WA. Epigenetic control of ctcfl/boris and oct4 expression in urogenital malignancies. Biochem Pharmacol 2006, 72: 1577–1588.
16. Woloszynska-Read A, James SR, Link PA, Yu J, Odunsi K and Karpf AR. DNA methylation-dependent regulation of boris/ctcfl expression in ovarian cancer. Cancer Immun 2007, 7: 21.
17. Kholmanskikh O, Loriot A, Brasseur F, De Plaen E and De Smet C. Expression of boris in melanoma: lack of association with mage-a1 activation. Int J Cancer 2008, 122: 777–784.
18. Pugacheva EM, Suzuki T, Pack SD, Kosaka-Suzuki N, Yoon J, Vostrov AA and Barsov E, *et al*. The structural complexity of the human boris gene in gametogenesis and cancer. PLoS One 2010, 5: e13872.
19. Chen K, Huang W, Huang B, Wei Y, Li B, Ge Y and Qin Y. Boris, brother of the regulator of imprinted sites, is aberrantly expressed in hepatocellular carcinoma. Genet Test Mol Biomarkers 2012, 17: 160–165.
20. Tiffen JC, Bailey CG, Marshall AD, Metierre C, Feng Y, Wang Q and Watson SL, *et al*. The cancer-testis antigen boris phenocopies the tumor suppressor ctcf in normal and neoplastic cells. Int J Cancer 2013, 133: 1603–1613.
21. Monk M, Hitchins M and Hawes S. Differential expression of the embryo/cancer gene ecsa(dppa2), the cancer/testis gene boris and the pluripotency structural gene oct4, in human preimplantation development. Mol Hum Reprod 2008, 14: 347–355.
22. Reya T, Morrison SJ, Clarke MF and Weissman IL. Stem cells, cancer, and cancer stem cells. Nature 2001, 414: 105–111.
23. Sell S. Stem cell origin of cancer and differentiation therapy. Crit Rev Oncol Hematol 2004, 51: 1–28.
24. Soltanian S and Matin MM. Cancer stem cells and cancer therapy. Tumour Biol 2011, 32: 425–440.
25. Clarke MF and Fuller M. Stem cells and cancer: two faces of eve. Cell 2006, 124: 1111–1115.
26. Santagata S, Ligon KL and Hornick JL. Embryonic stem cell transcription factor signatures in the diagnosis of primary and metastatic germ cell tumors. Am J Surg Pathol 2007, 31: 836–845.
27. Takahashi K, Tanabe K, Ohnuki M, Narita M, Ichisaka T, Tomoda K and Yamanaka S. Induction of pluripotent stem cells from adult human fibroblasts by defined factors. Cell 2007, 131: 861–872.
28. Takahashi K and Yamanaka S. Induction of pluripotent stem cells from mouse embryonic and adult fibroblast cultures by defined factors. Cell 2006, 126: 663–676.
29. Schoenhals M, Kassambara A, De Vos J, Hose D, Moreaux J and Klein B. Embryonic stem cell markers expression in cancers. Biochem Biophys Res Commun 2009, 383: 157–162.
30. Monk M and Holding C. Human embryonic genes re-expressed in cancer cells. Oncogene 2001, 20: 8085–8091.

31. Looijenga LH, Stoop H, de Leeuw HP, de Gouveia Brazao CA, Gillis AJ, van Roozendaal KE and van Zoelen EJ, *et al*. Pou5f1 (oct3/4) identifies cells with pluripotent potential in human germ cell tumors. Cancer Res 2003, 63: 2244–2250.
32. Li XL, Eishi Y, Bai YQ, Sakai H, Akiyama Y, Tani M and Takizawa T, *et al*. Expression of the sry-related hmg box protein sox2 in human gastric carcinoma. Int J Oncol 2004, 24: 257–263.
33. Tsukamoto T, Mizoshita T, Mihara M, Tanaka H, Takenaka Y, Yamamura Y and Nakamura S, *et al*. Sox2 expression in human stomach adenocarcinomas with gastric and gastric-and-intestinal-mixed phenotypes. Histopathology 2005, 46: 649–658.
34. Wong DJ, Liu H, Ridky TW, Cassarino D, Segal E and Chang HY. Module map of stem cell genes guides creation of epithelial cancer stem cells. Cell Stem Cell 2008, 2: 333–344.
35. Kang J, Shakya A and Tantin D. Stem cells, stress, metabolism and cancer: a drama in two octs. Trends Biochem Sci 2009, 34: 491–499.
36. Cole MD and Henriksson M. 25 years of the c-myc oncogene. Semin Cancer Biol 2006, 16: 241.
37. Ben-Porath I, Thomson MW, Carey VJ, Ge R, Bell GW, Regev A and Weinberg RA. An embryonic stem cell-like gene expression signature in poorly differentiated aggressive human tumors. Nat Genet 2008, 40: 499–507.
38. Rothenberg ME, Clarke MF and Diehn M. The myc connection: Es cells and cancer. Cell 2010, 143: 184–186.
39. Kim J, Woo AJ, Chu J, Snow JW, Fujiwara Y, Kim CG and Cantor AB, *et al*. A myc network accounts for similarities between embryonic stem and cancer cell transcription programs. Cell 2010, 143: 313–324.
40. Nagata S, Hirano K, Kanemori M, Sun LT and Tada T. Self-renewal and pluripotency acquired through somatic reprogramming to human cancer stem cells. PLoS One 2012, 7: e48699.
41. Renaud S, Loukinov D, Alberti L, Vostrov A, Kwon YW, Bosman FT and Lobanenkov V, *et al*. Boris/ctcfl-mediated transcriptional regulation of the htert telomerase gene in testicular and ovarian tumor cells. Nucleic Acids Res 2011, 39: 862–873.
42. Kosaka-Suzuki N, Suzuki T, Pugacheva EM, Vostrov AA, Morse HC, III, Loukinov D and Lobanenkov V. Transcription factor boris (brother of the regulator of imprinted sites) directly induces expression of a cancer-testis antigen, tsp50, through regulated binding of boris to the promoter. J Biol Chem 2011, 286: 27378–27388.
43. Recillas-Targa F, De La Rosa-Velazquez IA, Soto-Reyes E and Benitez-Bribiesca L. Epigenetic boundaries of tumour suppressor gene promoters: the ctcf connection and its role in carcinogenesis. J Cell Mol Med 2006, 10: 554–568.
44. Bhan S, Negi SS, Shao C, Glazer CA, Chuang A, Gaykalova DA and Sun W, *et al*. Boris binding to the promoters of cancer testis antigens, magea2, magea3, and magea4, is associated with their transcriptional activation in lung cancer. Clin Cancer Res 2011, 17: 4267–4276.
45. Hines WC, Bazarov AV, Mukhopadhyay R and Yaswen P. Boris (ctcfl) is not expressed in most human breast cell lines and high grade breast carcinomas. PLoS One 2010, 5: e9738.
46. Jones TA, Ogunkolade BW, Szary J, Aarum J, Mumin MA, Patel S and Pieri CA, *et al*. Widespread expression of boris/ctcfl in normal and cancer cells. PLoS One 2011, 6: e22399.
47. Rosa-Garrido M, Ceballos L, Alonso-Lecue P, Abraira C, Delgado MD and Gandarillas A. A cell cycle role for the epigenetic factor ctcf-l/boris. PLoS One 2012, 7: e39371.
48. Yawata T, Nakai E, Park KC, Chihara T, Kumazawa A, Toyonaga S and Masahira T, *et al*. Enhanced expression of cancer testis antigen genes in glioma stem cells. Mol Carcinog 2010, 49: 532–544.
49. Woloszynska-Read A, James SR, Song C, Jin B, Odunsi K and Karpf AR. Boris/ctcfl expression is insufficient for cancer-germline antigen gene expression and DNA hypomethylation in ovarian cell lines. Cancer Immun 2010, 10: 6.
50. Zendman AJ, Ruiter DJ and Van Muijen GN. Cancer/testis-associated genes: identification, expression profile, and putative function. J Cell Physiol 2003, 194: 272–288.
51. McBurney MW. P19 embryonal carcinoma cells. Int J Dev Biol 1993, 37: 135–140.
52. McBurney MW, Jones-Villeneuve EM, Edwards MK and Anderson PJ. Control of muscle and neuronal differentiation in a cultured embryonal carcinoma cell line. Nature 1982, 299: 165–167.
53. Xie Z, Tan G, Ding M, Dong D, Chen T, Meng X and Huang X, *et al*. Foxm1 transcription factor is required for maintenance of pluripotency of p19 embryonal carcinoma cells. Nucleic Acids Res 2010, 38: 8027–8038.
54. Solari M, Paquin J, Ducharme P and Boily M. P19 neuronal differentiation and retinoic acid metabolism as criteria to investigate atrazine, nitrite, and nitrate developmental toxicity. Toxicol Sci 2010, 113: 116–126.
55. Schoorlemmer J, Jonk L, Sanbing S, Van Puijenbroek A, Feijen A and Kruijer W. Regulation of oct-4 gene expression during differentiation of EC cells. Mol Biol Rep 1995, 21: 129–140.
56. Jones-Villeneuve EM, McBurney MW, Rogers KA and Kalnins VI. Retinoic acid induces embryonal carcinoma cells to differentiate into neurons and glial cells. J Cell Biol 1982, 94: 253–262.
57. Jones-Villeneuve EM, Rudnicki MA, Harris JF and McBurney MW. Retinoic acid-induced neural differentiation of embryonal carcinoma cells. Mol Cell Biol 1983, 3: 2271–2279.
58. Liu W and Saint DA. A new quantitative method of real time reverse transcription polymerase chain reaction assay based on simulation of polymerase chain reaction kinetics. Anal Biochem 2002, 302: 52–59.
59. Fan H and Robetorye RS. Real-time quantitative reverse transcriptase polymerase chain reaction. Methods Mol Biol 2010, 630: 199–213.
60. Livak KJ and Schmittgen TD. Analysis of relative gene expression data using real-time quantitative pcr and the 2(-delta delta c(t)) method. Methods 2001, 25: 402–408.
61. Xi J and Yang Z. Expression of raldhs (aldh1as) and cyp26s in human tissues and during the neural differentiation of p19 embryonal carcinoma stem cell. Gene Expr Patterns 2008, 8: 438–442.
62. Martin GR and Evans MJ. Differentiation of clonal lines of teratocarcinoma cells: formation of embryoid bodies *in vitro*. Proc Natl Acad Sci USA 1975, 72: 1441–1445.
63. Laplante I, Beliveau R and Paquin J. Rhoa/rock and cdc42 regulate cell-cell contact and n-cadherin protein level during neurodetermination of p19 embryonal stem cells. J Neurobiol 2004, 60: 289–307.
64. McBurney MW, Reuhl KR, Ally AI, Nasipuri S, Bell JC and Craig J. Differentiation and maturation of embryonal carcinoma-derived neurons in cell culture. J Neurosci 1988, 8: 1063–1073.
65. Niwa H, Miyazaki J and Smith AG. Quantitative expression of oct-3/4 defines differentiation, dedifferentiation or self-renewal of ES cells. Nat Genet 2000, 24: 372–376.
66. Loh YH, Wu Q, Chew JL, Vega VB, Zhang W, Chen X and Bourque G, *et al*. The oct4 and nanog transcription network regulates pluripotency in mouse embryonic stem cells. Nat Genet 2006, 38: 431–440.
67. Boiani M and Scholer HR. Regulatory networks in embryo-derived pluripotent stem cells. Nat Rev Mol Cell Biol 2005, 6: 872–884.
68. Chambers I, Colby D, Robertson M, Nichols J, Lee S, Tweedie S and Smith A. Functional expression cloning of nanog, a pluripotency sustaining factor in embryonic stem cells. Cell 2003, 113: 643–655.
69. Schoorlemmer J and Kruijer W. Octamer-dependent regulation of the kfgf gene in embryonal carcinoma and embryonic stem cells. Mech Dev 1991, 36: 75–86.
70. Tai MH, Chang CC, Kiupel M, Webster JD, Olson LK and Trosko JE. Oct4 expression in adult human stem cells: evidence in support of the stem cell theory of carcinogenesis. Carcinogenesis 2005, 26: 495–502.
71. Deb-Rinker P, Ly D, Jezierski A, Sikorska M and Walker PR. Sequential DNA methylation of the nanog and oct-4 upstream regions in human NT2

cells during neuronal differentiation. J Biol Chem 2005, 280: 6257–6260.
72. Rhee WJ and Bao G. Simultaneous detection of mrna and protein stem cell markers in live cells. BMC Biotechnol 2009, 9: 30.
73. Damjanov I, Cutler LS and Solter D. Ultrastructural localization of membrane phosphatases in teratocarcinoma and early embryos. Am J Pathol 1977, 87: 297–310.
74. Berstine EG, Hooper ML, Grandchamp S and Ephrussi B. Alkaline phosphatase activity in mouse teratoma. Proc Natl Acad Sci USA 1973, 70: 3899–3903.
75. Soudais C, Bielinska M, Heikinheimo M, MacArthur CA, Narita N, Saffitz JE and Simon MC, *et al*. Targeted mutagenesis of the transcription factor gata-4 gene in mouse embryonic stem cells disrupts visceral endoderm differentiation *in vitro*. Development 1995, 121: 3877–3888.
76. Arceci RJ, King AA, Simon MC, Orkin SH and Wilson DB. Mouse gata-4: a retinoic acid-inducible gata-binding transcription factor expressed in endodermally derived tissues and heart. Mol Cell Biol 1993, 13: 2235–2246.
77. Choi D, Lee HJ, Jee S, Jin S, Koo SK, Paik SS and Jung SC, *et al*. *In vitro* differentiation of mouse embryonic stem cells: enrichment of endodermal cells in the embryoid body. Stem Cells 2005, 23: 817–827.
78. Koike M, Sakaki S, Amano Y and Kurosawa H. Characterization of embryoid bodies of mouse embryonic stem cells formed under various culture conditions and estimation of differentiation status of such bodies. J Biosci Bioeng 2007, 104: 294–299.
79. Babuska V, Kulda V, Houdek Z, Pesta M, Cendelin J, Zech N and Pachernik J, *et al*. Characterization of p19 cells during retinoic acid induced differentiation. Prague Med Rep 2010, 111: 289–299.
80. McBurney MW and Rogers BJ. Isolation of male embryonal carcinoma cells and their chromosome replication patterns. Dev Biol 1982, 89: 503–508.
81. Laferrière NB and Brown DL. Expression and posttranslational modification of class III beta-tubulin during neuronal differentiation of p19 embryonal carcinoma cells. Cell Motil Cytoskeleton 1996, 35:188–199.
82. Mullen RJ, Buck CR and Smith AM. Neun, a neuronal specific nuclear protein in vertebrates. Development 1992, 116: 201–211.
83. Schwob AE, Nguyen LJ and Meiri KF. Immortalization of neural precursors when telomerase is overexpressed in embryonal carcinomas and stem cells. Mol Biol Cell 2008, 19: 1548–1560.
84. Kim KK, Adelstein RS and Kawamoto S. Identification of neuronal nuclei (neun) as fox-3, a new member of the fox-1 gene family of splicing factors. J Biol Chem 2009, 284: 31052–31061.
85. Sleutels F, Soochit W, Bartkuhn M, Heath H, Dienstbach S, Bergmaier P and Franke V, *et al*. The male germ cell gene regulator ctcfl is functionally different from ctcf and binds ctcf-like consensus sites in a nucleosome composition-dependent manner. Epigenetics Chromatin 2012, 5: 8.
86. Hart AH, Hartley L, Ibrahim M and Robb L. Identification, cloning and expression analysis of the pluripotency promoting nanog genes in mouse and human. Dev Dyn 2004, 230: 187–198.
87. Chen L and Daley GQ. Molecular basis of pluripotency. Hum Mol Genet 2008, 17: R23–R27.
88. Boyer LA, Lee TI, Cole MF, Johnstone SE, Levine SS, Zucker JP and Guenther MG, *et al*. Core transcriptional regulatory circuitry in human embryonic stem cells. Cell 2005, 122: 947–956.
89. Ben-Shushan E, Pikarsky E, Klar A and Bergman Y. Extinction of oct-3/4 gene expression in embryonal carcinoma × fibroblast somatic cell hybrids is accompanied by changes in the methylation status, chromatin structure, and transcriptional activity of the oct-3/4 upstream region. Mol Cell Biol 1993, 13: 891–901.
90. Minucci S, Botquin V, Yeom YI, Dey A, Sylvester I, Zand DJ and Ohbo K, *et al*. Retinoic acid-mediated down-regulation of oct3/4 coincides with the loss of promoter occupancy *in vivo*. EMBO J 1996, 15: 888–899.
91. Hattori N, Imao Y, Nishino K, Ohgane J, Yagi S, Tanaka S and Shiota K. Epigenetic regulation of nanog gene in embryonic stem and trophoblast stem cells. Genes Cells 2007, 12: 387–396.
92. Link PA, Zhang W, Odunsi K and Karpf AR. Boris/ctcfl mRNA isoform expression and epigenetic regulation in epithelial ovarian cancer. Cancer Immun 2013, 13: 6.
93. Narva E, Autio R, Rahkonen N, Kong L, Harrison N, Kitsberg D and Borghese L, *et al*. High-resolution DNA analysis of human embryonic stem cell lines reveals culture-induced copy number changes and loss of heterozygosity. Nat Biotechnol 2010, 28: 371–377.
94. Mastracci TL, Shadeo A, Colby SM, Tuck AB, O'Malley FP, Bull SB and Lam WL, *et al*. Genomic alterations in lobular neoplasia: a microarray comparative genomic hybridization signature for early neoplastic proliferationin the breast. Genes Chromosomes Cancer 2006, 45: 1007–1017.